

# An Exact Connection between $\pi$ and the Golden Ratio $\varphi$

Luis Teia

<sup>1</sup> von Karman Institute for Fluid Dynamics, Rhode-Saint-Genèse, Belgium

Correspondence: Dr Luis Teia, von Karman Institute for Fluid Dynamics, Chaussée de Waterloo 72, 1640 Rhode-Saint-Genèse, Belgium. E-mail: luisteia@sapo.pt

Received: March 15, 2022 Accepted: April 18, 2022 Online Published: May 9, 2022

doi:10.5539/jmr.v14n3p20

URL: <https://doi.org/10.5539/jmr.v14n3p20>

## Abstract

This article establishes a geometrical and mathematical bridge between the universal constant  $\pi$  and the golden ratio  $\varphi$  by interrelating the construction of the area of a circle using two approaches: one formed using the rotation of a regular unit pentagon and the other one from the rotation of its inverse — the pentagram of side reference  $\varphi$ . The mathematical end result is a linear expression of  $\pi$  as a function of  $\varphi$ . As an interesting side result, an expression for the area of a circle is derived based on the golden ratio  $\varphi$  and a geometrically motivated coefficient. A scripted program for the verification of the derived expressions is provided.

**Keywords:** Golden ratio, Pi, number theory, geometry, pentagon, pentagram, rotation

## 1. Introduction

The constant  $\pi$  and the golden ratio  $\varphi$  — arguably the two most known numbers in mathematics — hold a special place in the collective knowledge of humanity. Since the invention of the wheel, the universes of circularity (i.e., rotation) and linearity (i.e., translation) have been intertwined — implicitly and explicitly for the past millennia — by the constant  $\pi$  (Robson 2001, Swetz 2014). One definition presented in the 18<sup>th</sup> century defines  $\pi$  as the ratio of a circle's circumference to its diameter (Jones 1706). Using cunning ingenuity, humans have devised over time the cleverest ways to determine  $\pi$ , with more recently involving extraordinary computational methods to determine its 62.8 trillion digit (Lu 2021, Thomas 2021). While various complexities involving  $\pi$  have been unveiled — making it a practical tool in everyday science — its sister constant  $\varphi$  remains to a great extent a mystery. Its widespread practical application (to the same level as  $\pi$ ) is yet to be achieved. The golden ratio  $1:\varphi$  is a distinct mathematical property that is easily and recurrently observed in nature (Caryl-Sue 2012). It also appears (intentionally and unintentionally) on the architecture of great monuments — both ancient like the Parthenon and the Great Pyramids (Livio 2002), and more modern constructions such as for example the glass pyramid at the Louvre (which has a width to height ratio close to  $\varphi$ ) [Bernstein 1985]. More recently in astrophysics, the Kepler space telescope has discovered a group of stars that has a ratio between pulsing frequencies close to the irrational number  $0.61803398875 = 1/\varphi$ , which is the inverse of the golden number  $\varphi = 1.61803398875$  (Moskowitz, 2015). Another discovery in the field of quantum physics suggests that hidden quantum resonant symmetries exist in the ferromagnetic properties of solid-state matter carrying frequencies interrelated by the golden number (Coldea 2022). Pure mathematical studies have also been conducted on  $\varphi$  geometrical origins (Rigby 1988). The golden ratio has been observed in various aspects of human anatomy, with particular emphasis in aesthetics (Singh 2019, Castro 2021). For example, in biology the shape of human red blood cells has been shown to be linked to the negative of the golden ratio (Zhang 2017). The relative size of bones in a human hand presents proportions in line with the golden ratio, while the human ear presents an approximate shape to the golden spiral (Persaud 2015). In the works of Leonardo da Vinci (Murtinho 2015), the iconic drawing of a human being inside a circle — representing circularity being governed by  $\pi$  — and a square — representing linearity holding various golden proportions  $1:\varphi$  — precludes the existence of a relation between these two constants, where the human in itself is implied philosophically as being the connection between them. Despite the substantial amount of research on both  $\pi$  and  $\varphi$ , no account has been found in where these two constants are expressed with respect to one another. There are several possible benefits that such linkage can bring. For example, it will be possible to express the properties of a circle — perimeter or area — as a function of the golden number (in this instance, the case for area will be later derived from first principles). Similarly, properties from phenomena in nature governed by the golden spiral (such as the sunflower) could be expressed as a function of  $\pi$ . The ability to express  $\pi$  as a function of the golden ratio  $\varphi$ , and vice versa, would potentially bridge circular patterns (e.g., shapes/orbits of planets/stars, atoms, etc) to those behaving in a spiral manner (e.g., shape of a galaxy, whirlpools, etc). This encompasses the possibility that the aforementioned star

pulsating frequency ratio governed by  $\varphi$  (as observed by the Kepler space telescope) could potentially be related to the circular  $\pi$  properties of the planet-star system, like the circumference/volume of the stars or the types of orbits of the planets surrounding them.

## 2. Hypothesis

The hypothesis of this article is that there is a geometrical construct, from which both the constant  $\pi$  and the golden ratio  $\varphi$  can be determined or measured independently, that acts as a foundation allowing for the formulation of a mathematical expression by which constant  $\pi$  becomes a function of the golden ratio  $\varphi$ , and vice versa.

## 3. Theory

Establishing a common ground between the constant  $\pi$  and the golden ratio  $\varphi$  implies the existence of a geometrical construct that, when formed, exhibits in its definition both quantities. The constant  $\pi$  implies a circle [formed by the rotation of regular pentagons, as explained in a preceding work (Teia 2022)], while  $\varphi$  is found explicitly in a pentagram. Hence, a way to bring the two constants into one geometrical expression is by rotating both the pentagon and its associated pentagram such that they form the same circle. Consider five angularly equidistant (by angle  $5\delta$ ) points A, B, C, D and E at an equal radial distance from the center (Figure 1). Connecting each point with its neighbor gives a pentagon of side unit (Figure 1a). Connecting each alternating point gives a pentagram of side equal to the golden ratio  $\varphi = (1 + \sqrt{5})/2 = 1.618033989$  (Figure 1b). Figure 1a shows the rotating five pentagons forming the approximate area of a ring — defined by an inner and outer circle — whose interference forms a series of strips (highlighted in green). Figure 1b shows the same process but executed with a pentagram instead. Both circles — in Figure 1a and 1b — have the same area  $A_{\odot}$ . If the pentagon between the points ABCDE has a reference length side unit  $1(=AE)$ , it implies the presence of  $\pi$ , or more precisely the value relative to a pentagon of  $\pi_{108^\circ} = \pi_{90^\circ} \tan(180/5)$ , which holds an internal angle of  $108^\circ$  (Teia 2022) — then the pentagram formed between the same points A, B, C, D and E has a reference length  $\varphi(=AD)$ . In both cases, the circles are scalable by multiplying the reference length with  $L$ . If in both Figures 1a and 1b the outer circle becomes the inner, a new ring is formed downscaled from the first. The process is repeated in a fractal manner inward until the entire area of both circles is filled. Adding the areas of the individual rings gives the area of the circle. Each approach yields a different equation to determine the same circle area. Equating the areas results in a connection that allows the formulation of  $\pi$  directly as a function of  $\varphi$ . When the pentagon is rotated with equal angular distance, the interference pattern formed results in a series of identical strips AB'H (as shown in Figure 1a and 1b). This approach of finding the area of a circle using rotating polygons follows closely from a previously publication (Teia 2022).

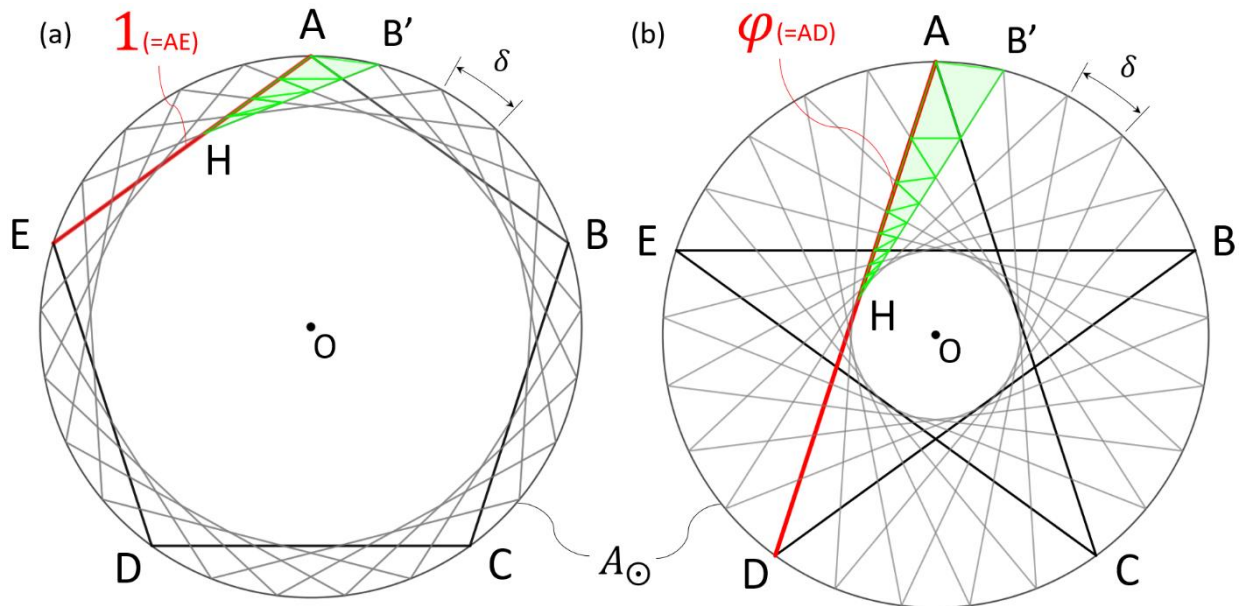


Figure 1. Ring formed by five evenly spaced revolving: (a) pentagons and (b) pentagrams

### 3.1 Circle Area as a Function of $\pi$

The sum of all the strips AB'H (in Figure 1a) defines the outer ring of the circle, and gives an initial approximation to the ring's area. A closer zoom into a single strip in Figure 2a is shown in Figure 2b. Here, the side of the regular pentagon  $AE = L = 1$  is subdivided into segments by the rotating pentagon copies, with the sum of the

different parts give the equality

$$2(x_1 + x_2 + x_3 + x_4) + z_5 = 1 \equiv L \quad (1)$$

While scaling the circle area is possible by changing the value of  $L$ , for the purpose of determining  $\pi$ , it is convenient to set  $L$  as unit. Here the longest side of the triangles composing the strip is defined as variable  $z$ , with the shorter being variable  $x$ . A more general expression for Eq.(1) with infinite number of pentagons ( $N = \infty$ ) will be presented later. Looking along the segment  $AE$ , it is noticeable that its partition is symmetric about its midpoint, explaining the presence of the multiplication factor two in Eq.(1).

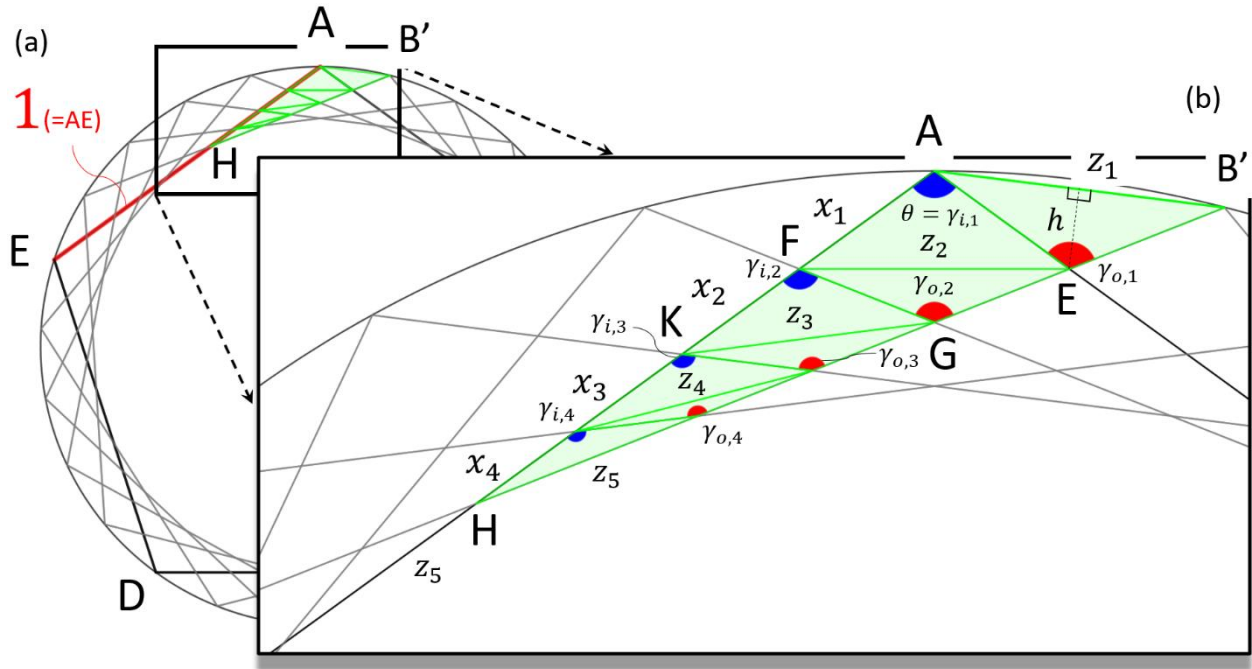


Figure 2. Interference strip created by five revolving pentagons: (a) overview and (b) key lengths and angles

A program was scripted in the open-source software Octave (Eaton et al 2021) containing the mathematical process herein described. This can be found in Annex A, and can be copied and ran directly in the “Editor” tab. The angles and lengths necessary for quantifying the area of the triangles are identified by zooming into the interference strip  $AB'H$  (Figure 2b). The strip is formed by pairs of adjacent outward and inward facing triangles, where each pair is located along the strip by index  $n$  (starting outside and moving inwards). The successive angles of the triangles facing outwards are given by

$$\gamma_{o,n} = \theta + (n)\delta \quad (2)$$

where  $\theta = 180^\circ - 360^\circ/N$  is the polygon internal angle, and the subscript  $o$  denotes an obtuse angle facing outward away from the center of the circle (starting with the most outer triangle  $AB'E$  at  $n = 1$ ). Similarly, the successive angles of the triangles facing inwards are given by

$$\gamma_{i,n} = \theta + (n-1)\delta = \gamma_{o,n-1} \quad (3)$$

and the subscript  $i$  denotes an obtuse angle facing inward towards the center of the circle (starting with the most outer triangle  $AEF$  at  $n = 1$ ). The sides  $x$  and  $z$  are in fact interconnected and interdependent via the law of cosines. When applied between two adjacent triangles at the same level — like  $AB'E$  and  $AEF$ , both at  $n = 1$  — establishes a connection between two successive values of  $z$ . The following relation is present for triangle  $AB'E$

$$x_1^2 - 2x_1x_1 \cos \gamma_{o,1} + x_1^2 = z_1^2 \quad (4)$$

All trigonometric functions in this research operate directly on an argument specified in degrees. Applying to triangle  $AEF$ , the associated relation between lengths and angles becomes

$$x_1^2 - 2x_1x_1 \cos \gamma_{i,1} + x_1^2 = z_2^2 \quad (5)$$

Since Eq.(4) and Eq.(5) have the common variable  $x_1$ , they can be equated resulting in the simplified relation

$$z_2 = \frac{\sqrt{1 - \cos \gamma_{i,1}}}{\sqrt{1 - \cos \gamma_{o,1}}} z_1 \quad (6)$$

Generalizing further to a relation between two subsequent lengths  $z_n$  and  $z_{n+1}$  [with simultaneous expansion using Eq.(2) and Eq.(3)], results in

$$z_{n+1} = \frac{\sqrt{1 - \cos \gamma_{i,n}}}{\sqrt{1 - \cos \gamma_{o,n}}} z_n = \frac{\sqrt{1 - \cos(\theta + (n-1)\delta)}}{\sqrt{1 - \cos(\theta + n\delta)}} z_n = Q_n z_n \quad (7)$$

A connection between two successive values of  $x$  is achieved when the law of cosines is applied between two adjacent triangles at different levels — like AEF at  $n = 1$  and GEF at  $n = 2$ . Starting with triangle GEF, the relation becomes

$$x_2^2 - 2x_2x_1 \cos \gamma_{o,2} + x_1^2 = z_2^2 \quad (8)$$

Both Eq.(8) and the former relation for triangle AEF [in Eq.(5)] have the common variable  $z_2$ , that when combined give

$$x_2 = \frac{\sqrt{1 - \cos \gamma_{i,1}}}{\sqrt{1 - \cos \gamma_{o,2}}} x_1 \quad (9)$$

This is both generalized and further expanded [by replacing Eq.(2) and Eq.(3)], resulting in

$$x_{n+1} = \frac{\sqrt{1 - \cos \gamma_{i,n}}}{\sqrt{1 - \cos \gamma_{o,n+1}}} x_n = \frac{\sqrt{1 - \cos(\theta + (n-1)\delta)}}{\sqrt{1 - \cos(\theta + n\delta)}} x_n = K_n x_n \quad (10)$$

We can now expand Eq.(1) by replacing both Eq.(7) and Eq.(10), resulting in

$$2(1 + K_1 + K_1K_2 + K_1K_2K_3)x_1 + (Q_4Q_3Q_2Q_1)z_1 = 1 \quad (11)$$

Further re-arranging, while replacing Eq.(4) in the form  $z_1 = x_1 \sqrt{2(1 - \cos \gamma_{o,1})}$  gives

$$x_1(P = 5) = \frac{1}{2(1 + K_1 + K_1K_2 + K_1K_2K_3) + (Q_4Q_3Q_2Q_1)\sqrt{2(1 - \cos \gamma_{o,1})}} \quad (12)$$

The resulting expression for  $z_1$  becomes

$$z_1(P = 5) = \frac{\sqrt{2(1 - \cos \gamma_{o,1})}}{2(1 + K_1 + K_1K_2 + K_1K_2K_3) + (Q_4Q_3Q_2Q_1)\sqrt{2(1 - \cos \gamma_{o,1})}} \quad (13)$$

Both Eq.(12) and Eq.(13) are applicable to the particular case of five revolving unit pentagons, while the general case of  $z_1$  for any number of rotating pentagons  $P$  extrapolates to

$$z_1(P) = \frac{\sqrt{2(1 - \cos \gamma_{o,1})}}{2[1 + \sum_{m=1}^{P-2} \prod_{n=1}^m (K_n)] + \prod_{n=1}^{P-1} (Q_n) \sqrt{2(1 - \cos \gamma_{o,1})}} \quad (14)$$

While at the same time, the generalized function for  $x_1$  for any number of pentagons is

$$x_1(P) = \frac{1}{2[1 + \sum_{m=1}^{P-2} \prod_{n=1}^m (K_n)] + \prod_{n=1}^{P-1} (Q_n)} \sqrt{2(1 - \cos \gamma_{o,1})} \quad (15)$$

Equations (14) and (15) can be seen at work in the annexed Octave program, in the form of two for-loop cycles (lines 20 to 34). Knowing firstly  $x_1$  [from Eq.(12)] and  $z_1$  [from Eq.(13)], it is possible — using Eq.(7) and Eq.(10) — to obtain values for the general expressions of  $x_n$  and  $z_n$  (programmed in Annex A as lines 35 to 40). Having expressions for the various sides of the triangles allows the computation of their areas. For example, the area  $A_{o,1}$  of the triangle AB'E (in the strip AB'H) is given as

$$A_{o,1} = h \times \frac{z_1}{2} \quad \text{with} \quad h = \sqrt{x_1^2 - \frac{z_1^2}{2}} \quad (16)$$

Thus, resulting in the areas  $A_{o,1}$  of triangle ABC and  $A_{i,1}$  of triangle ACD (both at radial position  $n = 1$ ) as

$$A_{o,1} = \frac{z_1}{2} \sqrt{x_1^2 - \frac{1}{4} z_1^2} \quad ; \quad A_{i,1} = \frac{z_2}{2} \sqrt{x_1^2 - \frac{1}{4} z_2^2} \quad (17)$$

While it is more interesting to discuss the triangles in their inward and outward orientation, mathematically it is more convenient to lump them into one expression. Thus, the area in the strip is given by a double sum that accounts for the contributions of all the pairs (one inward and one outward) triangles, resulting in

$$A_{strip}(N = 5) = \sum_{i=1}^{P-1} \sum_{j=1}^2 \frac{z_{i+j-1}}{2} \sqrt{x_i^2 - \frac{1}{4} z_{i+j-1}^2} \quad (18)$$

A ring is formed as a result of the summation of  $N \times P$  strips— henceforth identified as the most outward ring. For the case of five revolving pentagons, the area of the ring is expressed as the sum of their individual  $5 \times P$  strip areas, resulting in

$$A_{ring}(N = 5) = (5 \times P) \left\{ \sum_{i=1}^{P-1} \sum_{j=1}^2 \frac{z_{i+j-1}}{2} \sqrt{x_i^2 - \frac{1}{4} z_{i+j-1}^2} \right\} \quad (19)$$

To understand how the area inside the outer ring is formed, consider Figure 3a that shows a more detailed example of a ring formed by the interference of sixteen pentagons at an angular equidistance to each other, defining an area webbed by their interference pattern. The rest of the area inside the inner circle can be filled with similar rings, leading to a complete tessellation of the area of the circle. As an illustration, consider the simple case of just two pentagons (colored in black within the outer ring), one upright and one inverted. Uniting the midpoints — I and J — along their sides forms a smaller pair of pentagons, whose sides have a length interlinked geometrically to the first by the triangle DIJ. The process is fractal, and when repeated leads to a convergence towards the center (as shown in Figure 3a). Subsequently, this process of fractalization can be applied to each of the sixteen pentagons in the outer ring, leading to the tessellation of an infinite number of inward rings (shown in Figure 3b), and thus of the entire area of the circle. The length of the side of a pentagon is related to its immediate lower fractal expression by a factor of  $2 \times [1/2 \cos(36^\circ)] = \cos(36^\circ)$  — that is, the angle between the sides of two pentagons of adjacent levels is  $\varepsilon = (180^\circ - 108^\circ)/2 = 36^\circ$  — that results in an area relation of  $\cos^2(36^\circ)$ . This means that multiplying this factor by the area of the outer ring gives the area of the next adjacent inward ring. Multiplying it again, gives the next inward ring, and so on and so forth. The end result is a sum of products, where each product term is a scaling factor transforming the area of the outer ring into an inward ring at a specific level (e.g., two fractal levels down, the product becomes  $\cos^4(36^\circ)$ ).

$$\cos^2(36^\circ) + \cos^4(36^\circ) + \cos^8(36^\circ) + \dots = \sum_{k=1}^{\infty} \cos^{2^k}(36^\circ) \quad (20)$$

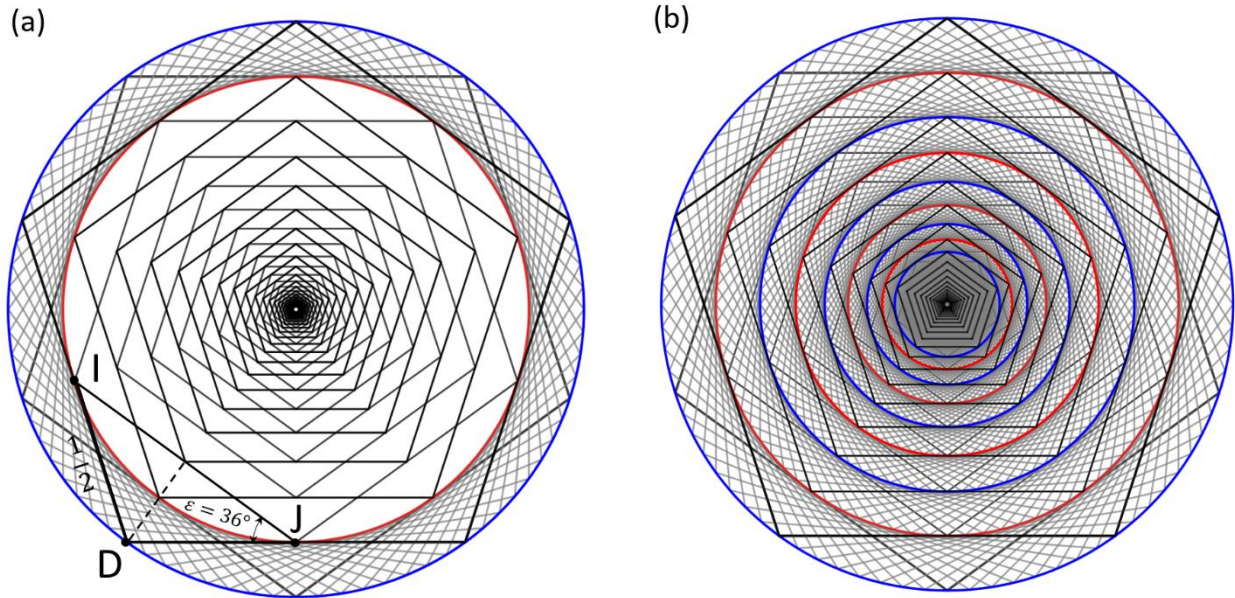


Figure 3. Fractal approach using the infinite inward propagation of (a) 2 pentagons and (b) 16 pentagons

For numerical simplicity (in working out a first example), let us resume the original case of five revolving pentagons only. The sum of all the area of all the rings is obtained by multiplying the outer ring area [given by Eq.(19)] by the series of scaling factors [given by Eq.(20)], resulting in

$$A_{\odot}(N=5) = (5 \times P) \left\{ \sum_{i=1}^{P-1} \sum_{j=1}^2 \frac{z_{i+j-1}}{2} \sqrt{x_i^2 - \frac{1}{4} z_{i+j-1}^2} \right\} \times \sum_{k=1}^{\infty} \cos^{2k}(36^\circ) \quad (21)$$

The area of the circle is computed by substituting the values in Table 1 into Eq.(21) resulting in 2.181413566546808, which is just an initial estimate achieved using only five revolving pentagons (Figure 4). One way to ascertain the validity of Eq.(21) is by corroborating it against a numerically determined value using a Computer-Aided Design program — of which open-source software Geogebra (Feng 2014) and FreeCAD (Havre 2021) are examples. When the number of pentagons reaches two million, the estimated area becomes 2.2732777998(45238), which matches the CAD value (2.273277799898968) up to ten decimal places.

Table 1. Properties of the triangles composing the strip in the outer ring (pentagon approach)

Angle $\gamma$		Side $z$	Side $x$	Area $A_o$
(Outward)	(Inward)			(Outward)
$\gamma_{1o} = \mathbf{90^\circ}$	$\gamma_{1i} = 60^\circ$	$z_1 = 0.21322963$	$x_1 = 0.12166382$	$A_{o,1} = 0.00624891$
$\gamma_{2o} = \mathbf{120^\circ}$	$\gamma_{2i} = 90^\circ$	$z_2 = 0.19685619$	$x_2 = 0.10586211$	$A_{o,2} = 0.00383579$
$\gamma_{3o} = \mathbf{150^\circ}$	$\gamma_{3i} = 120^\circ$	$z_3 = 0.18553534$	$x_3 = 0.09577667$	$A_{o,3} = 0.00220960$
$\gamma_{4o} = \mathbf{150^\circ}$	$\gamma_{4i} = 120^\circ$	$z_4 = 0.178101792$	$x_4 = 0.08975867$	$A_{o,4} = 0.00100180$
		$z_5 = 0.17387747$		
Area $A_i$	(Inward)			
$A_{i,1} = \mathbf{0.00703881}$ ; $A_{i,2} = \mathbf{0.00473110}$ ; $A_{i,3} = \mathbf{0.00313973}$ ; $A_{i,4} = \mathbf{0.00194065}$				

It was shown in a previous work (Teia 2022) that the ratio between the area of a circle (corresponding to the inner circle in Figure 1a) and the polygon circumscribing it (corresponding to the pentagon of side  $1=AB$ ) is equal to the ratio of the relative value of  $\pi$  (that for a pentagon is  $\pi_{108^\circ} = 4.324031329886049$ ) divided by the number of sides of the polygon (i.e.,  $N = 5$  for a pentagon). Like peeling layers from an onion, transforming the inner circle area into the outer circle area simply requires the addition of an outer ring.



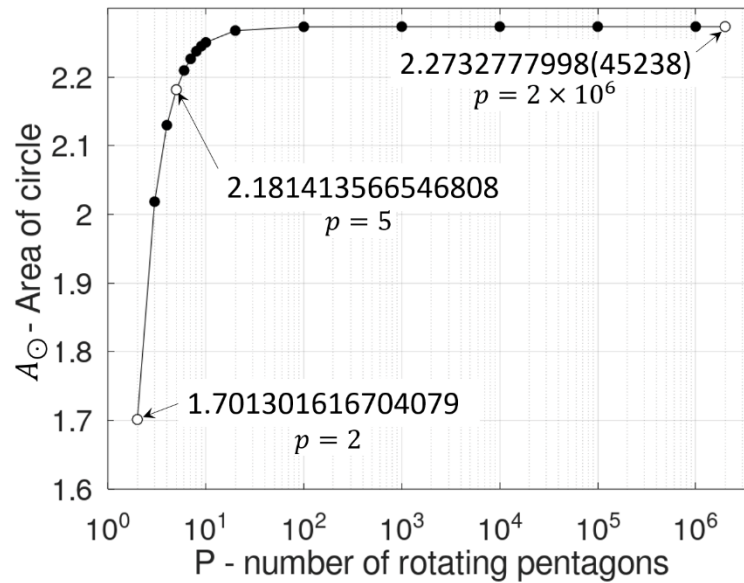


Figure 4. Accuracy of the predicted area of circle  $A_{\odot}$  for varying number of interfered rotating pentagons

From the perspective of Eq.(20), this is achieved by dividing the aforementioned area of the inner circle by a scaling factor  $\cos^2(36^\circ)$  (instead of multiplication, which would reduce the area of the rings inwardly). A recent published work (Teia 2022) showed that the numerical approximation given by Eq.(21) corresponds (at infinity) to the exact value given by

$$A_{\odot}(N=5) = \left\{ \frac{\pi_{108^\circ}}{5} \frac{5(1^2)}{4\sqrt{5-2\sqrt{5}}} \right\} \frac{1}{\cos^2(36^\circ)} = 2.273277799899 \quad (22)$$

### 3.2 Circle Area as a Function of $\varphi$

The process here is essentially the same (as in section 3.1), except that the pentagons are replaced by five-pointed stars or pentagrams, and the reference length of the series is now  $\varphi - 1$ . Figure 5a shows five angularly-equidistant pentagrams, which forms twenty-five identical interference strips. For convenience, the zoom into the strip in Figure 5b has been rotated 90 degrees clockwise. The strip's orientation does not really matter, as it is an angularly recurrent feature that exists all around the circle.

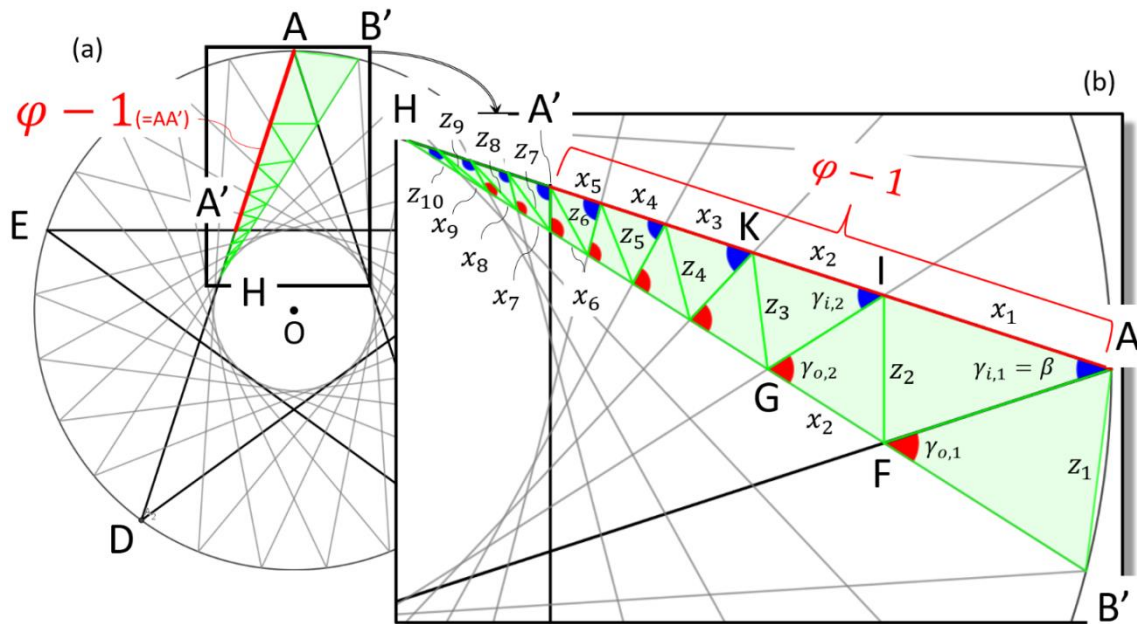


Figure 5. Interference strip created by five revolving pentagrams: (a) overview and (b) key lengths and angles

The inward triangles are facing right to left towards the center, while the outward triangles are facing left to right away from the center. The internal angle of the triangles facing outward away from the centre is given as

$$\gamma_{o,n} = \beta + (n)\delta \quad (23)$$

where  $n$  is the triangle pair (inward and outward) counting from right to left, and the angles are  $\beta = 180^\circ/5 = 36^\circ$  and  $\delta = 360/(N \times P) = 360/25 = 14.4^\circ$ . In turn, the internal angle of the triangles facing inward is

$$\gamma_{i,n} = \beta + (n-1)\delta = \gamma_{o,n-1} \quad (24)$$

In Figure 5b, side  $x_2$  (in triangle IFG) relates to side  $x_1$  (in triangle AEI) via the law of cosines (as both have the common side  $z_2$ )

$$x_2 = \frac{\sqrt{1 - \cos \gamma_{i,1}}}{\sqrt{1 - \cos \gamma_{o,2}}} x_1 \quad (25)$$

A program was scripted in the open-source software Octave (Eaton et al 2021) containing the mathematical process herein described. This can be found in Annex B, and can be copied and ran directly in the “Editor” tab. Hence in general, any side  $x_{n+1}$  is connected to its predecessor  $x_n$  (and hence also to the initial  $x_1$ ) via the law of cosines. The equation can be further developed by replacing the outward and inward facing angles —  $\gamma_{o,n+1}$  from Eq.(23) and  $\gamma_{i,n}$  from Eq.(24) — resulting in

$$x_{n+1} = \frac{\sqrt{1 - \cos \gamma_{i,n}}}{\sqrt{1 - \cos \gamma_{o,n+1}}} x_n = \frac{\sqrt{1 - \cos(\beta + (n-1)\delta)}}{\sqrt{1 - \cos(\beta + (n+1)\delta)}} x_n = K_n x_n \quad (26)$$

The distance AA' is always fixed with the position of the pentagram ACEBD, so what changes is the number of times it partitions due to the other revolving pentagrams. In this case, the segment AA' of length  $\varphi - 1$  is split in five times by the superimposed revolving pentagrams. This relation (in Figure 5b) is expressed as

$$x_1 + x_2 + x_3 + x_4 + x_5 = \varphi - 1 \quad (27)$$

Remembering that all lengths  $x$  are relatable to the initial  $x_1$  via the law of cosines given by Eq.(26) results in

$$x_1 + (K_1)x_1 + (K_2.K_1)x_1 + (K_3.K_2.K_1)x_1 + (K_4.K_3.K_2.K_1)x_1 = \varphi - 1 \quad (28)$$

Re-arranging this expression for  $x_1$  to be a function of  $\varphi - 1$  gives

$$x_1 = \frac{\varphi - 1}{1 + K_1 + K_2.K_1 + K_3.K_2.K_1 + K_4.K_3.K_2.K_1} = \bar{x}_1(\varphi - 1) \quad (29)$$

This means that Eq.(26) can also be reduced to

$$x_{n+1} = \bar{x}_{n+1}(\varphi - 1) \quad (30)$$

where the normalized length  $\bar{x}_{n+1}$  is given as

$$\bar{x}_{n+1} = \frac{1}{1 + K_1 + K_2.K_1 + K_3.K_2.K_1 + K_4.K_3.K_2.K_1} \quad (31)$$

For triangle AB'F, the law of cosines establishes a relation between  $z_1$  and the (now known)  $x_1$  via the outward facing angle  $\gamma_{o,1}$  as

$$x_1^2 - 2x_1x_1 \cos \gamma_{o,1} + x_1^2 = z_1^2 \quad (32)$$

This gives an expression for  $z_1$

$$z_1 = x_1 \sqrt{2(1 - \cos \gamma_{o,1})} \quad (33)$$

which can be further expanded by replacing  $x_1$  from Eq.(30) and Eq.(31)

$$z_1 = \frac{\sqrt{2(1 - \cos \gamma_{o,1})}}{1 + K_1 + K_2.K_1 + K_3.K_2.K_1 + K_4.K_3.K_2.K_1} (\varphi - 1) = \bar{z}_1(\varphi - 1) \quad (34)$$



While Eq.(29) and Eq.(34) are applicable to the particular case of five revolving unit pentagrams, the general case of  $z_1$  for any number of rotating squares is extrapolated to

$$z_1(P) = \frac{\sqrt{2(1 - \cos \gamma_{o,1})}}{1 + \sum_{m=1}^{P-1} \prod_{n=1}^m (K_n)} (\varphi - 1) \quad (35)$$

while the generalized function for  $x_1$  being inherently

$$x_1(P) = \frac{\varphi - 1}{1 + \sum_{m=1}^{P-1} \prod_{n=1}^m (K_n)} \quad (36)$$

Similarly, any side  $z_{n+1}$  is connected to its predecessor  $z_n$  (and hence also to the initial  $z_1$ ) via the law of cosines. The equation can be further developed by replacing the outward and inward facing angles —  $\gamma_{o,n}$  from Eq.(23) and  $\gamma_{i,n}$  from Eq.(24) — resulting in

$$z_{n+1} = \frac{\sqrt{1 - \cos \gamma_{i,n}}}{\sqrt{1 - \cos \gamma_{o,n}}} z_n = \frac{\sqrt{1 - \cos(\beta + (n-1)\delta)}}{\sqrt{1 - \cos(\beta + n\delta)}} z_n = \bar{z}_{n+1}(\varphi - 1) \quad (37)$$

The same process as in section 1.2 applies here. The expression that defines the areas of the triangles that composes the strip is the same as the one defined previously in Eq.(17). As such, the double sum that defined the area of the strip in Eq.(18) is modified by normalized Eq.(30) and Eq.(37) to become

$$A_{strip}(N=5) = \sum_{i=1}^{P-1} \sum_{j=1}^2 \frac{\bar{z}_{i+j-1}}{2} \sqrt{\bar{x}_i^2 - \frac{1}{4} \bar{z}_{i+j-1}^2} \times (\varphi - 1)^2 \quad (38)$$

From Eq.(38), the normalized expression for the area of the outer ring in Eq.(19) becomes

$$A_{ring}(N=5) = (5 \times P) \left\{ \sum_{i=0}^{P-1} \sum_{j=1}^2 \frac{\bar{z}_{i+j-1}}{2} \sqrt{\bar{x}_i^2 - \frac{1}{4} \bar{z}_{i+j-1}^2} \right\} \times (\varphi - 1)^2 \quad (39)$$

Here, the modeling of the fractality differs from the previous section 3.2. The lengths of the sides of two pentagrams belonging to different adjacent fractal levels are interrelated by triangle DIJ (Figure 6a).

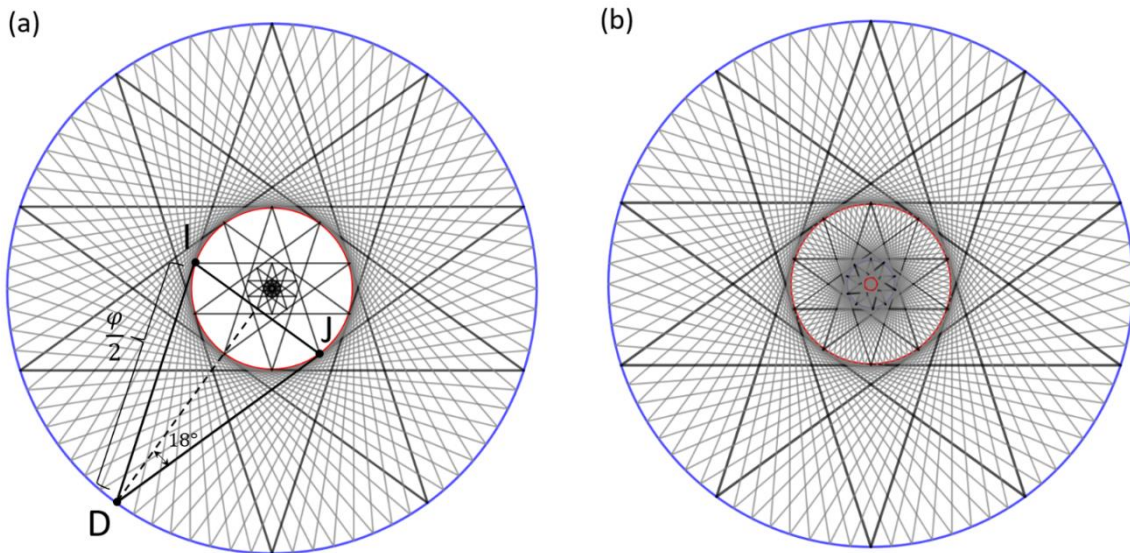


Figure 6. Fractal approach using the infinite inward propagation of (a) 2 pentagrams and (b) 16 pentagrams

The outer most pentagram has an half side of  $DI = DJ = \varphi/2$ , and the projection of both (DI and DJ) onto the side of the pentagram belonging to the next fractal level gives  $IJ = \varphi \sin(18^\circ)$ . This results in areas between two adjacent fractal levels being interrelated by the scaling factor  $\sin^2(18^\circ)$ . When accounting for all the subsequent rings, their area

reduction compounds by multiplying each subsequent level by  $\sin^2(18^\circ)$ . The entire area contribution for all rings is accounted for by adding these area factors as a sum

$$\sin^2(18^\circ) + \sin^4(18^\circ) + \sin^8(18^\circ) + \dots = \sum_{k=1}^{\infty} \sin^{2k}(18^\circ) \quad (40)$$

This multiplies the area of the outer ring Eq.(39) to give the total area of all the internal rings summed together, which is in the end the area of the entire circle (Figure 6b), resulting in

$$A_{\odot}(N=5) = (5 \times P) \left\{ \sum_{i=1}^{P-1} \sum_{j=1}^2 \frac{\bar{z}_{i+j-1}}{2} \sqrt{\bar{x}_i^2 - \frac{1}{4} \bar{z}_{i+j-1}^2} \right\} \times \sum_{k=1}^{\infty} \sin^{2k}(18^\circ) (\varphi - 1)^2 \quad (41)$$

The novelty in Eq.(41) is that the area of the circle is defined as a function of the golden ratio  $\varphi$  (without the presence of  $\pi$ ). Scaling of the circle, and its area, is achieved by multiplying the reference length by variable  $L$ , that in this case works by replacing the length  $(\varphi - 1)$  by  $(\varphi - 1)L$  [where  $L$  is a scalar that increases or decreases the side of the pentagram]. The area of the circle is computed by substituting the values from Table 2 into Eq.(41) resulting in 2.245631227704724, which is an initial estimate based upon only five rotating pentagrams (as indicated in Figure 7). When the number reaches two million, the estimate becomes 2.273277799(900334), matching the CAD value (2.273277799898968) up to nine decimal places.

Table 2. Properties of the triangles composing the strip in the outer ring (pentagram approach)

Angle $\gamma$		Side $z$	Side $x$	Area $A$
(Outward)	(Inward)			(Outward)
$\gamma_{1o} = \mathbf{50.4^\circ}$	$\gamma_{1i} = 36.0^\circ$	$z_1 = 0.21322963$	$x_1 = 0.25039925$	$A_{o,1} = 0.02415551$
$\gamma_{2o} = \mathbf{64.8^\circ}$	$\gamma_{2i} = 50.4^\circ$	$z_2 = 0.15475525$	$x_2 = 0.14440790$	$A_{o,2} = 0.00943447$
$\gamma_{3o} = \mathbf{79.2^\circ}$	$\gamma_{3i} = 64.8^\circ$	$z_3 = 0.12297179$	$x_3 = 0.96459964$	$A_{o,3} = 0.00456986$
$\gamma_{4o} = \mathbf{93.6^\circ}$	$\gamma_{4i} = 79.2^\circ$	$z_4 = 0.10337167$	$x_4 = 0.70902686$	$A_{o,4} = 0.00250864$
$\gamma_{5o} = \mathbf{108^\circ}$	$\gamma_{5i} = 93.6^\circ$	$z_5 = 0.90390145$	$x_5 = 0.55864182$	$A_{o,5} = 0.00148403$
$\gamma_{6o} = \mathbf{122.4^\circ}$	$\gamma_{6i} = 108^\circ$	$z_6 = 0.81446472$	$x_6 = 0.46471443$	$A_{o,6} = 0.00091170$
$\gamma_{7o} = \mathbf{136.8^\circ}$	$\gamma_{7i} = 122.4^\circ$	$z_7 = 0.75192375$	$x_7 = 0.40435726$	$A_{o,7} = 0.00055963$
$\gamma_{8o} = \mathbf{151.2^\circ}$	$\gamma_{8i} = 136.8^\circ$	$z_8 = 0.70868193$	$x_8 = 0.36583433$	$A_{o,8} = 0.00032238$
$\gamma_{9o} = \mathbf{165.6^\circ}$	$\gamma_{9i} = 151.2^\circ$	$z_9 = 0.68028831$	$x_9 = 0.34284761$	$A_{o,9} = 0.00014616$
		$z_{10} = 0.66415284$		
Area A		(Inward)		
$A_{i,1} = \mathbf{0.01842700}$ ; $A_{i,2} = \mathbf{0.00803400}$ ; $A_{i,3} = \mathbf{0.00420949}$ ; $A_{i,4} = \mathbf{0.00246907}$ ;				
$A_{i,5} = \mathbf{0.00155732}$ ; $A_{i,6} = \mathbf{0.00102695}$ ; $A_{i,7} = \mathbf{0.00069026}$ ; $A_{i,8} = \mathbf{0.00045808}$ ;				
$A_{i,9} = \mathbf{0.00028314}$				

### 3.3 Connection between $\pi$ and $\varphi$

As a major outcome, there are two expressions — Eq.(22) and Eq.(41) — to compute the area of a circle, both created using similar approaches and adopting different geometrical references. The first approach expresses it as a function of  $\pi$ , while the second as a function of  $\varphi$ . Equating the two expressions establishes a relation between these two constants, resulting in

$$\pi_{108^\circ} \frac{L^2}{4\sqrt{5-2\sqrt{5}}} \frac{1}{\cos^2(36^\circ)} = \lim_{P \rightarrow \infty} (5P) \left\{ \sum_{i=1}^{P-1} \sum_{j=1}^2 \frac{\bar{z}_{i+j-1}}{2} \sqrt{\bar{x}_i^2 - \frac{1}{4} \bar{z}_{i+j-1}^2} \right\} \times \sum_{k=1}^{\infty} \sin^{2k}(18^\circ) (\varphi - 1)^2 \quad (42)$$

In a previous mathematical research work (Teia 2022), it was found that a relative value of function  $\pi_\theta$  is obtained when the polygon circumscribing the circle changes from a square (that is linked to the typical concept of orthogonality, with side equal to the diameter) as to another polygon (where  $\theta$  is the internal angle of the polygon).

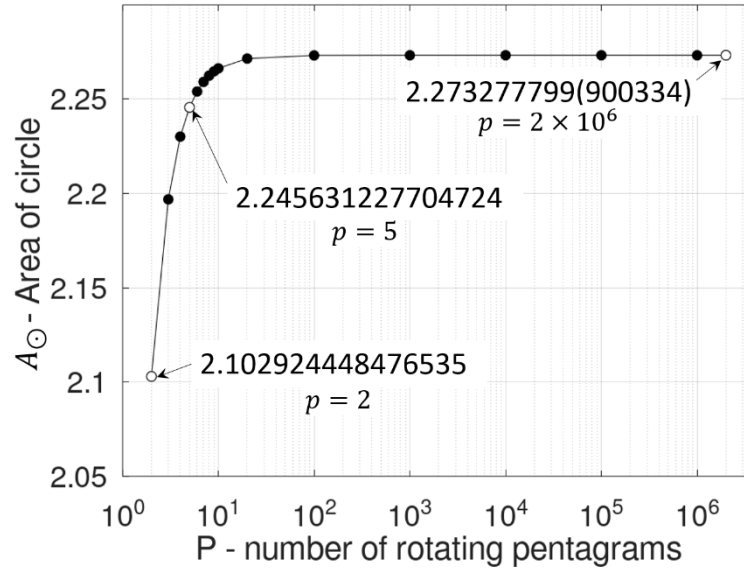


Figure 7. Accuracy of the predicted area of circle  $A_{\odot}$  for varying number of interfered rotating pentagrams

In the present work, the selected polygon is a pentagon (due to the presence of  $\varphi$  inherent in its star configuration as a pentagram), and for which the value of the function becomes  $\pi_{108^\circ} = 4.2340313299$  [in the same manner as  $\pi_{90^\circ} = 3.1415926535$  was obtained when using a square during prior work (Teia 2022)]. In general, the relativity of the function  $\pi_\theta$  to the selected circle-circumscribing polygon follows the subsequent rule

$$\pi_\theta = \pi_{90^\circ} \tan\left(\frac{\theta}{2}\right) \quad (43)$$

where  $N$  is the number of sides of the polygon used (in the case of a pentagon,  $N = 5$ ). Replacing Eq.(43) into the left hand side of Eq.(42) gives

$$\pi_{90^\circ} \tan\left(\frac{108}{2}\right) \frac{1}{4\sqrt{5-2\sqrt{5}}} \frac{1}{\cos^2(36^\circ)} = \lim_{P \rightarrow \infty} (5P) \left\{ \sum_{i=1}^{P-1} \sum_{j=1}^2 \frac{\bar{z}_{i+j-1}}{2} \sqrt{\bar{x}_i^2 - \frac{1}{4} \bar{z}_{i+j-1}^2} \right\} \times \sum_{k=1}^{\infty} \sin^{2k}(18^\circ) (\varphi - 1)^2 \quad (44)$$

The square term on the right containing  $\varphi$  can be expanded and simplified into a linear term as

$$(\varphi - 1)^2 = \varphi^2 - 2\varphi + 1 = (1 + \varphi) - 2\varphi + 1 = 2 - \varphi \quad (45)$$

Replacing this back into Eq.(44), while moving the terms multiplying  $\pi (= \pi_{90^\circ})$  to the right as denominators, gives

$$\pi = \frac{\lim_{P \rightarrow \infty} (5P) \left\{ \sum_{i=1}^{P-1} \sum_{j=1}^2 \frac{\bar{z}_{i+j-1}}{2} \sqrt{\bar{x}_i^2 - \frac{1}{4} \bar{z}_{i+j-1}^2} \right\} \times \sum_{k=1}^{\infty} \sin^{2k}(18^\circ)}{\tan\left(\frac{108}{2}\right) \frac{1}{4\sqrt{5-2\sqrt{5}}} \frac{1}{\cos^2(36^\circ)}} (2 - \varphi) \quad (46)$$

Concluding, Eq.(46) can be simply written as a linear relation between  $\pi$  and  $\varphi$  defined as

$$\pi = \Phi(2 - \varphi) \quad (47)$$

where  $\Phi$  is a geometrical coefficient (expressing the ratio of normalized areas given by the pentagon and pentagram rotation approaches) that is only dependent on the state of refinement of the two meshes (that are defining the same reference circle). A program that executes Eq.(46) in the open-source software Octave is available in Annex C (which is a modified version of Annex B). Concluding, for two infinitely perfect meshes — that is, when the number of pentagons and pentagrams tends to infinity —  $\Phi$  converges to the constant 8.224796346, providing an exact (traceable geometrical and mathematical) connection between  $\pi$  and the golden ratio  $\varphi$ .

## References

- Bailey, D. H., & Borwein, J. (2014). Pi Day Is Upon Us Again and We Still Do Not Know if Pi Is Normal. *American Mathematical Monthly*, 121(3), 187-278. <https://doi.org/10.4169/amer.math.monthly.121.03.191>
- Bernstein, R. (1985). I. M. Pei's Pyramid: A Provocative Plan for The Louvre. *The New York Times*. Retrieved from <https://www.nytimes.com/1985/11/24/magazine/im-pei-s-pyramid-a-provative-plan-for-the-louvre.html>
- Caryl-Sue. (2012). The Golden Ratio. *National Geographic Society. Resource Library*. Retrieved from <https://www.nationalgeographic.org/media/golden-ratio/>
- Castro, J. (2021). How the Brain Responds to Beauty. *Scientific American*. Retrieved from <https://www.scientificamerican.com/article/how-the-brain-responds-to-beauty/>
- Coldea, R., Tennant, D. A., Wheeler, E. M., Wawrzynska, E., Prabhakaran, D., Telling, M., Habicht, K., & Kiefer, K. (2010). Quantum Criticality in an Ising Chain: Experimental Evidence for Emergent E8 Symmetry. *Science*, 327(5962), 177-180. <https://doi.org/10.1126/science.1180085>
- Eaton, J. W., Bateman, D., Hauberg, S., & Wehbring, R. (2021). *GNU Octave: A high-level interactive language for numerical computations*. Retrieved from <https://octave.org/octave.pdf>
- Feng, G. T. (2013). *Introduction to Geogebra – Version 4.4*. Retrieved from [https://www.academia.edu/34890249/Introduction\\_to\\_Introduction\\_to\\_GeoGebra](https://www.academia.edu/34890249/Introduction_to_Introduction_to_GeoGebra)
- Jones, W. (1706). *Synopsis Palmariorum Matheseos: or, a New Introduction to the Mathematics*. pp. 243, 263. Retrieved from <https://archive.org/details/SynopsisPalmariorumMatheseosOrANewIntroductionToTheMathematics>
- Keller, T., Mundani, Ralf-Peter, Rölke, H., & Schmidt, M. (2021). World record attempt by UAS Grisons: Pi-Challenge. *University of Applied Sciences Grisons*. Retrieved from <https://www.fhgr.ch/en/specialist-areas/applied-future-technologies/davis-centre/pi-challenge/>
- Livio, M. (2002). *The Golden Ratio: The Story of Phi, the World's Most Astonishing Number*. Broadway Books. New York.
- Lu, D. (2021). New mathematical record: what's the point of calculating pi? *The Guardian*. Retrieved from <https://www.theguardian.com/science/2021/aug/17/new-mathematical-record-whats-the-point-of-calculating-pi>
- Moskowitz, C. (2015). Strange Stars Pulsate According to the Golden Ratio. *Scientific American*. Retrieved from <https://www.scientificamerican.com/article/strange-stars-pulsate-according-to-the-golden-ratio/>
- Murtinho, V. (2015). Leonardo's Vitruvian Man Drawing: A New Interpretation Looking at Leonardo's Geometric Constructions. *Nexus Network Journal*, 17, 507–524. <https://doi.org/10.1007/s00004-015-0247-7>
- Persaud, D., and O'Leary, P. D. (2015). Fibonacci Series, Golden Proportions, and the Human Biology. *Austin Journal of Surgery*, 2(5), 1066.
- Rigby, J. F. (1988). Equilateral triangles and the golden ratio. *The Mathematical Gazette*, 72(459), 27–30. <https://doi.org/10.2307/3617983>
- Robson, E. (2001) Neither Sherlock Holmes nor Babylon: A Reassessment of Plimpton 322. *Historia Mathematica*, 28, 167-206. <https://doi.org/10.1006/hmat.2001.2317>
- Singh, P., Vijayan, R., & Mosahebi, A. (2019). The Golden Ratio and Aesthetic Surgery. *Aesthetic Surgery Journal*, 39(1), NP4–NP5. <https://doi.org/10.1093/asj/sjy240>
- Swetz, F. J. (2014). Mathematical Treasure: Old Babylonian Area Calculation. *Convergence*. <https://doi.org/10.4169/loci003954>
- Teia, L. (2022). Relativity of  $\pi$  as a Function of the Rotation of N-sided Unit Polygons. *Journal of Mathematics Research*, 14(2). <https://doi.org/10.5539/jmr.v14n2p19>
- van Havre, Y. et al. (2021). "FreeCAD - A Manual". Retrieved from <https://freecadweb.org/manual/a-freecad-manual.pdf>
- Zhang, X., & Ou-Yang, Z. (2017). Mechanism behind the Beauty: The Golden Ratio Appeared in the Shape of Red Blood Cells. *Communications in Computational Physics*, 21(2), 559–569. <https://doi.org/10.4208/cicp.OA-2016-0205>

**Annex A**

```
clc, clear
```

```
% SETUP
```

```
format long % Increases decimal place output
```

```
N=5; % Sides of pentagon
```

```
p=100000; % Number of pentagons % Line 5
```

```
if p>10 probe=0; else probe=1; end % Enable extra details
```

```
display('PENTAGON Approach -->> function of Pi')
```

```
display('--- Sides in a pentagon and number revolving'), display(N), display(p)
```

```
display('--- Angle per sector (degrees)'), delta=360/(N*p)
```

```
display('--- Internal angle of pentagon (degrees)'), theta=180-360/N % Line 10
```

```
display('--- Area scaling factor due to fractality'), f=cosd(180/N)^2
```

```
display('--- Area of the N-sided unit regular pentagon'), Apoly=[N/(4*tand(180/N))]
```

```
% SIDES X(N) and Z(N)
```

```
display('--- Sides of most outward triangle in the strip')
```

```
for i=1:(p-1) % Line 15
```

```
    Q(i)=sqrt(1-cosd(theta+(i-1)*delta))/sqrt(1-cosd(theta+(i)*delta));
```

```
    if i~=(p-1)
```

```
        K(i)=sqrt(1-cosd(theta+(i-1)*delta))/sqrt(1-cosd(theta+(i+1)*delta));
```

```
end end
```

```
sQ=prod(Q); sK(1)=1; % Line 20
```

```
for m=1:(p-2)
```

```
    sK(m+1)=prod(K(1:m));
```

```
end
```

```
x=1/(2*(sum(sK)+sQ*sqrt(2*(1-cosd(theta+delta))))); x1=x(1)
```

```
z=x1*sqrt(2*(1-cosd(theta+delta))); z1=z(1) % Line 25
```

```
for v=1:(p-1)
```

```
    z(v+1)=sqrt(1-cosd(((theta)+(v-1)*delta))/sqrt(1-cosd(theta+(v)*delta))*z(v);
```

```
    if v~=(p-1)
```

```
        x(v+1)=sqrt(1-cosd(((theta)+(v-1)*delta))/sqrt(1-cosd(theta+(v+1)*delta))*x(v);
```

```
    else x=x(1:v); % Line 30
```

```
end end
```

```
if probe==1
```

```
    display('--- Sides of subsequent triangles'), display(z); display(x);
```

```
end
```

```
% AREAS : TRIANGLE, STRIP & FIRST RING % Line 35
```

```
s=0; l=0;
```

```
for i=1:(p-1)
```

```
    for j=1:2
```

```
        s=s+1; At(s)=z(i+j-1)/2*sqrt(x(i)^2-1/4*z(i+j-1)^2);
```

```
end end % Line 40
```

```
if probe==1 disp('--- Area of each triangle in outward strip'); disp(At) end
```

```

display('--- Area of most outward strip'), As=sum(At)
display('--- Area of most outward ring'), Ar=As*(N*p)
% FRACTAL SCALING SUM OF RINGS
SumScale=0; % Starting variable for loop % Line 45
n=1000; % Number of inward rings considered (ideally infinite)
for k=1:n
SumScale=SumScale+f^k; % Formation of the series
end
display('--- Scaling series due to inward fractality'), Fseries=SumScale % Line 50
if probe==1 disp('Scaling series'); disp(Fseries) end
% APPROX. AREA OF CIRCLE
display('--- Area of circle');
Ac=Ar*Fseries
% RATIO OF AREAS % Line 55
display('--- Ratio of areas circle/polygon'), Ratio=Ac/Apoly
% FUNCTION PI FOR SELECTED POLYGON
display('--- Value of Pi (for the chosen polygon)'), PiN=Ratio*N

```

## Annex B

```

clc, clear
% SETUP
format long % Increases decimal place output
N=5; % Sides of pentagram
p=100000; % Number of pentagrams % Line 5
if p>10 probe=0; else probe=1; end % Enable extra details
% Identification of approach
disp('PENTAGRAM Approach -->> function of Phi'); phi=(1+sqrt(5))/2
disp('--- Number of revolving pentagrams'); disp(p)
disp('--- Angle per sector (degrees)'); delta=360/(N*p) % Line 10
disp('--- Internal angle of pentagram (degrees)'); theta=180-360/N; beta=180/N
disp('--- Area scaling factor due to fractality'); f=sind(180/(2*N))^2
% ANGLES GAMMA INWARD & OUTWARD
for v=1:((2*p)-1)
    gammaO(v)=beta+(v)*delta;    gammaI(v)=beta+(v-1)*delta; % Line 15
end
if probe==1
    disp('--- Angles of triangles, both inward and outward facing')
    disp('Inward facing angles (deg):'); disp(gammaI); disp('Outward facing angles (deg):'); disp(gammaO)
end % Line 20
% SIDES X(N) and Z(N)
disp('--- Factors K')
for v=1:(p-1)

```



```

    K(v)=sqrt(1-cosd(gammaI(v)))/sqrt(1-cosd(gammaO(v+1)));
end % Line 25
if probe==1 disp(K) end
disp('--- Sides of most outward triangle in the strip')
Q(1)=1;
for v=1:(p-1)
    Q(v+1)=Q(v)*K(v); % Line 30
end
x(1)=[1/sum(Q)]*(phi-1); x1=x(1) % This is when PHI is introduced in the equation
z(1)=x(1)*sqrt(2*(1-cosd(gammaO(1)))); z1=z(1)
for v=1:((2*p)-1)
    z(v+1)=sqrt(1-cosd(((beta))+(v-1)*delta))/sqrt(1-cosd(beta+(v)*delta))*z(v); % Line 35
    if v~=((2*p)-1)
        x(v+1)=sqrt(1-cosd(((beta))+(v-1)*delta))/sqrt(1-cosd(beta+(v+1)*delta))*x(v);
    else x=x(1:v);
end end
disp('--- Sides of subsequent triangles'); % Line 40
if probe==1 disp('z(n)'); disp(z); disp('x(n)'); disp(x); end
% AREAS : TRIANGLE, STRIP & FIRST RING
s=0; l=0;
for i=1:((2*p)-1)
    for j=1:2 % Line 45
        s=s+1; At(s)=z(i+j-1)/2*sqrt(x(i)^2-1/4*z(i+j-1)^2);
    end end
if probe==1 disp('--- Area of each triangle in outward strip'); disp(At) end
disp('--- Area of most outward strip'); As=sum(At)
disp('--- Area of most outward ring'); Ar=As*(N*p) % Line 50
% FRACTAL SCALING SUM OF RINGS
SumScale=1; % Starting variable for loop
n=1000; % Number of inward rings considered (ideally infinite)
for k=1:n
    SumScale=SumScale+f^k; % Formation of the series % Line 55
end
disp('--- Scaling series due to inward fractality'); Fseries=SumScale
if probe==1 disp('Scaling series'); disp(Fseries) end
% APPROX. AREA OF CIRCLE
disp('--- Area of circle') % Line 60
Ac=Ar*Fseries

```

## Annex C

```

clc, clear
% SETUP

```

```

format long % Increases decimal place output
N=5; % Sides of pentagram
p=100000; % Number of pentagrams % Line 5
if p>10 probe=0; else probe=1; end % Enable extra details
% Identification of approach
disp('EQUATION 44 CONNECTING PI TO PHI'); Phi=(1+sqrt(5))/2
disp('--- Number of revolving pentagrams'); disp(p)
disp('--- Angle per sector (degrees)'); delta=360/(N*p) % Line 10
disp('--- Internal angle of pentagram (degrees)'); theta=180-360/N; beta=180/N
disp('--- Area scaling factor due to fractality'); f=sind(180/(2*N))^2
% ANGLES GAMMA INWARD & OUTWARD
for v=1:((2*p)-1)
    gammaO(v)=beta+(v)*delta;    gammaI(v)=beta+(v-1)*delta; % Line 15
end
if probe==1
    disp('--- Angles of triangles, both inward and outward facing')
    disp('Inward facing angles (deg):'); disp(gammaI); disp('Outward facing angles (deg):'); disp(gammaO)
end % Line 20
% SIDES X(N) and Z(N)
disp('--- Factors K')
for v=1:(p-1)
    K(v)=sqrt(1-cosd(gammaI(v)))/sqrt(1-cosd(gammaO(v+1)));
end % Line 25
if probe==1 disp(K) end
disp('--- Sides of most outward triangle in the strip')
Q(1)=1;
for v=1:(p-1)
    Q(v+1)=Q(v)*K(v); % Line 30
end
x(1)=1/sum(Q); x1=x(1)
z(1)=x(1)*sqrt(2*(1-cosd(gammaO(1)))); z1=z(1)
for v=1:((2*p)-1)
    z(v+1)=sqrt(1-cosd(((beta)+(v-1)*delta)))/sqrt(1-cosd(beta+(v)*delta))*z(v); % Line 35
    if v~=((2*p)-1)
        x(v+1)=sqrt(1-cosd(((beta)+(v-1)*delta)))/sqrt(1-cosd(beta+(v+1)*delta))*x(v);
    else x=x(1:v);
end end
disp('--- Sides of subsequent triangles'); % Line 40
if probe==1 disp('z(n)'); disp(z); disp('x(n)'); disp(x); end
% AREAS : TRIANGLE, STRIP & FIRST RING
s=0; l=0;
for i=1:((2*p)-1)

```

```

    for j=1:2 % Line 45
        s=s+1; At(s)=z(i+j-1)/2*sqrt(x(i)^2-1/4*z(i+j-1)^2);
    end end
    if probe==1 disp('--- Area of each triangle in outward strip'); disp(At) end
    disp('--- Area of most outward strip'); As=sum(At)
    disp('--- Area of most outward ring'); Ar=As*(N*p) % Line 50
    % FRACTAL SCALING SUM OF RINGS
    SumScale=1; % Starting variable for loop
    n=1000; % Number of inward rings considered (ideally infinite)
    for k=1:n
        SumScale=SumScale+f^k; % Formation of the series % Line 55
    end
    disp('--- Scaling series due to inward fractality'); Fseries=SumScale
    if probe==1 disp('Scaling series'); disp(Fseries) end
    % APPROX. AREA OF CIRCLE
    disp('--- Area of circle') % Line 60
    Ac=Ar*Fseries
    % FIND OMEGA
    disp('--- Coefficient Omega');
    Omega=Ac/(tand(theta/2)*1/(4*sqrt(5-2*sqrt(5)))*1/(cosd(36))^2)
    % PI BASED ON PHI % Line 65
    disp('--- Constant Pi');
    Pi=Omega*(2-Phi)

```

### Copyrights

Copyright for this article is retained by the author(s), with first publication rights granted to the journal.

This is an open-access article distributed under the terms and conditions of the Creative Commons Attribution license (<http://creativecommons.org/licenses/by/4.0/>).